Inorganic Chemistry

Article

pubs.acs.org/IC

Dimensionality of Intermolecular Interactions in Layered Crystals by Electronic-Structure Theory and Geometric Analysis

Janine George,[†] Volker L. Deringer,[†] and Richard Dronskowski*[,†,‡]

[†]Institute of Inorganic Chemistry, Chair of Solid-State and Quantum Chemistry, RWTH Aachen University, Landoltweg 1, 52056 Aachen, Germany

[‡]Jülich-Aachen Research Alliance (JARA-HPC), RWTH Aachen University, 52056 Aachen, Germany

Supporting Information

ABSTRACT: Two-dimensional (2D) and layered structures gained a lot of attention in the recent years ("post-graphene era"). The chalcogen cyanides $S(CN)_2$ and $Se(CN)_2$ offer themselves as interesting model systems to study layered inorganic crystal structures; both are built up from cyanide molecules connected by chalcogen bonds (ChBs). Here, we investigate ChBs and their cooperativity directly *within* the layers of the $S(CN)_2$ and $Se(CN)_2$ crystal structures and, furthermore, in putative $O(CN)_2$ and $Te(CN)_2$ crystal structures derived therefrom. Moreover, we determine the energetic contributions of ChBs *within* the layers to the overall stabilization energy. To compare these structures not only energetically but also geometrically, we derive a direction-dependent root mean square of the Cartesian displacement, a possible tool for further computational investigations of layered compounds. The molecular chains connected by ChBs are highly cooperative but do *not* influence each other when combined to layers: the ChBs are nearly orthogonal in terms of energy when connected to the same chalcogen acceptor atom. Layers built up from ChBs account for 41% to 79% of the overall interaction energy in the crystal. This provides new, fundamental insight into the meaning of ChBs, and therefore directed intermolecular interactions, for the stability of crystal structures.

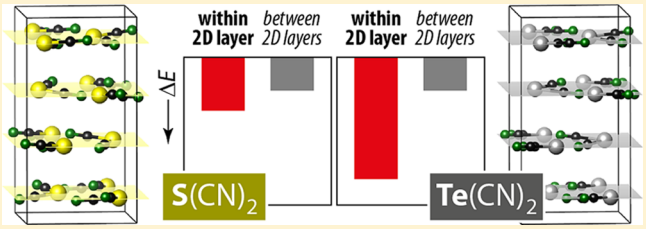

INTRODUCTION

Recent synthetic advances and fascinating physical properties have led to a surge of interest in "two-dimensional" (2D) and layered materials.[1] Graphene[2,3] and silicene[4,5] and, more recently, germanene[6] and phosphorene[7,8] are experimentally observed elemental allotropes that extend in two directions; pertinent multinary examples include transition-metal chalcogenides[9] and layered tellurides.[10] In fact, these materials are all but new; on the contrary, they have a long-standing history in solid-state and inorganic chemistry. Take layered MoS_2: crystal-structure reports go back to Pauling in 1923,[11] its crystals were already investigated regarding the thickness and number of layers in the 1960s,[12] and layered MoS_2 has now been rediscovered in today's post-graphene era.[13]

Sometimes, three-dimensional (3D) crystal structures show quasi-2D dimensionality in their electronic structure, as seen by Feng et al.[14] in high-pressure density functional theory (DFT) calculations on Li_xBe_{1-x} compounds. These revealed an electronic density of states (DOS) with a steplike feature—that is, a nearly constant DOS (E)—at the bottom of the valence band, indicative of quasi-2D dimensionality in the electronic structure. Moreover, John D. Corbett *to whom this work is dedicated* has found 2D dimensionality of metal−metal bonding with the help of overlap populations in tellurides.[15]

In recent contributions, King et al. and Schlüter et al. have stressed that the concept of 2D structures can be extended to molecular and organic crystals as well.[16,17] It is crucial to understand these 2D molecular crystals in detail, a quest that is now, likewise, experimentally well-founded. The traditional concept of band dispersion, however, cannot be applied to molecular crystals because (save for very short and strong hydrogen bonds; cf. ref 18) these show no significant covalent nature *between* their molecular building blocks. Instead, "weak" interactions such as hydrogen[19] and halogen bonds[20,21] are important for molecular crystals and their stability. Formally, these interactions can be extended to include chalcogen,[22] pnictogen,[23] and carbon bonds,[24] as they are sometimes called, and they can all be traced back to electrostatic and dispersive interactions.[25−28] They are defined as the attraction of a less electronegative hydrogen, halogen, chalcogen, pnictogen, or carbon atom X with an electronegative partner D.[29] In the case of the well-known halogen bond, the less electronegative atom X, thereby, is covalently bound to a neighboring atom Y and has a formal noble-gas electronic configuration:

$$\mathrm{Y}-\overset{\delta+}{\mathrm{X}}\cdots\overset{\delta-}{\mathrm{D}}$$

In the context of crystal structures, the mutual influence that intermolecular interactions have onto each other has been investigated. An important concept is that of cooperativity, i.e.,

Special Issue: To Honor the Memory of Prof. John D. Corbett

Received: September 27, 2014
Published: November 3, 2014

   dx.doi.org/10.1021/ic5023328 | *Inorg. Chem.* 2015, 54, 956−962

bonds amplifying each other, which is observed in hydrogen- and halogen-bonded and even chalcogen- and pnictogen-bonded systems and also in systems with combinations of these bonds.[30−42] Recently, we have investigated chalcogen-bond (ChB) cooperativity in one-dimensional (1D) chains by first-principles computations with true periodic boundary conditions.[43]

In contrast to the above viewpoint of mostly localized intermolecular interactions as the driving force for stability, Dunitz and Gavezzotti have argued that less localized interactions between molecules play a crucial role also.[44] Depending on the particular system at hand, one or the other may have the more relevant role, and the *entirety* of the system must be looked upon, rather than a handful of isolated contacts. Studying interactions in periodic systems by appropriate (DFT-D) total-energy computations provides an attractive tool in this regard because they allow one to capture both effects in an ab initio framework.

Here, we contribute new arguments to this important discussion. We use ab initio simulations to partition cyanide crystals into infinite fragments such as chains and layers and calculate the interaction energies in these lower-dimensional fragments. This scheme has previously been developed by our laboratory.[43,45,46] The idea behind the present work is to quantify the interaction energy in a set of simple and well-characterized layered crystal structures; on purpose, we have chosen systems that bridge the gap between molecular and "classical" solid-state inorganic chemistry.

THEORETICAL SECTION

Quantum-Chemical Calculations. We performed electronic-structure calculations based on DFT with the Vienna ab initio simulation package.[47−50] The generalized gradient approximation functional of Perdew, Burke, and Ernzerhof (PBE)[51] and the projector augmented-wave (PAW) method[52,53] were applied. Moreover, a dispersion correction was used, namely, the D3 correction by Grimme et al.[54] The latter showed promising results with molecular crystals, even for a "more quantitative understanding",[55] and it has already successfully been used for the quantification of ChB energies.[27] Calculations of isolated molecules as well as 1D and 2D fragments were performed with a supercell approach that we have used before.[43,45,46] Thereby, at least 20 Å of vacuum was inserted perpendicular to the extended chains or layers such as to uphold translational symmetry. The interaction energy ΔE_{int} was calculated as follows:

$$\Delta E_{\text{int}} = E_{\text{crystal/fragment}} - \sum E_{\text{monomer}} \tag{1}$$

$E_{\text{crystal/fragment}}$ is the energy of the crystal, layer, chain, or other fragment in focus. E_{monomer} is the energy of the monomer cut out from the crystal, layer, chain, or other fragment, obtained in the same DFT framework. Our definition is such that negative values indicate stabilizing interactions. In addition, phonon calculations were performed using the finite-displacement method,[56] as implemented in PHONOPY.[57]

New Structural Descriptor. To compare substituted crystal structures, a quantitative measure for structural similarity seems beneficial. We build upon the definition of the Cartesian displacement d_i* of van de Streek and Neumann:[58]

$$d_i^* = \frac{1}{2}(|\mathbf{G}_1(r_{1_i} - r_{2_i})| + |\mathbf{G}_2(r_{1_i} - r_{2_i})|) \tag{2}$$

Thereby, $\mathbf{G}_1$ and $\mathbf{G}_2$ are transformation matrices from fractional to Cartesian coordinates for structures 1 and 2. r_{1_i} and r_{2_i} are the fractional coordinates of an atom i in structures 1 and 2, respectively. This concept is very useful because one can assess the correctness of experimental crystal structures.[58] Here, we will extend the previous definition to incorporate dimensionality to the picture, specifically with layered inorganic materials in mind.

Instead of building the arithmetic mean of the absolute Cartesian displacement in each coordinate system, we first build the arithmetic mean of the coordinate systems and calculate the absolute Cartesian displacement d_i with this mean. This definition of the Cartesian displacement is limited by d_i* in the definition of van de Streek and Neumann[58] (triangle inequality):

$$\begin{aligned} d_i &= \frac{1}{2}|(\mathbf{G}_1 + \mathbf{G}_2)(r_{1_i} - r_{2_i})| \\ &\le \frac{1}{2}(|\mathbf{G}_1(r_{1_i} - r_{2_i})| + |\mathbf{G}_2(r_{1_i} - r_{2_i})|) \end{aligned} \tag{3}$$

This definition allows us to vectorize the Cartesian displacement:

$$\mathbf{d}_i = \begin{pmatrix} d_{x_i} \\ d_{y_i} \\ d_{z_i} \end{pmatrix} = \frac{\mathbf{G}_1 + \mathbf{G}_2}{2}(r_{1_i} - r_{2_i}) \tag{4}$$

Now, a root mean square (rms) of the Cartesian displacement can easily be defined for each direction separately:

$$\begin{pmatrix} \text{rms}_x \\ \text{rms}_y \\ \text{rms}_z \end{pmatrix} = \begin{pmatrix} \sqrt{\frac{\sum_{i=1}^{n} d_{x_i}^2}{n}} \\ \sqrt{\frac{\sum_{i=1}^{n} d_{y_i}^2}{n}} \\ \sqrt{\frac{\sum_{i=1}^{n} d_{z_i}^2}{n}} \end{pmatrix} \tag{5}$$

This direction-dependent rms value is related to the total one:

$$\text{rms} = \sqrt{\text{rms}_x^2 + \text{rms}_y^2 + \text{rms}_z^2} \tag{6}$$

It is also limited by the rms* defined by van de Streek and Neumann,[58] as we show here for completeness:

$$\begin{aligned} \text{rms} &= \sqrt{\text{rms}_x^2 + \text{rms}_y^2 + \text{rms}_z^2} \\ &= \sqrt{\left(\sqrt{\frac{\sum_{i=1}^{n} d_{x_i}^2}{n}}\right)^2 + \left(\sqrt{\frac{\sum_{i=1}^{n} d_{y_i}^2}{n}}\right)^2 + \left(\sqrt{\frac{\sum_{i=1}^{n} d_{z_i}^2}{n}}\right)^2} \\ &= \sqrt{\frac{\sum_{i=1}^{n} d_{x_i}^2}{n} + \frac{\sum_{i=1}^{n} d_{y_i}^2}{n} + \frac{\sum_{i=1}^{n} d_{z_i}^2}{n}} \\ &= \sqrt{\frac{\sum_{i=1}^{n} d_{x_i}^2 + d_{y_i}^2 + d_{z_i}^2}{n}} = \sqrt{\frac{\sum_{i=1}^{n} d_i^2}{n}} \\ &\le \text{rms}^* = \sqrt{\frac{\sum_{i=1}^{n} d_i^{*2}}{n}} \end{aligned} \tag{7}$$

dx.doi.org/10.1021/ic5023328 | Inorg. Chem. 2015, 54, 956−962

RESULTS AND DISCUSSION

From Chains to Layers: Chalcogen-Bonded Model Systems. In our recent publication,[43] we investigated chains linked by different categories of intermolecular interactions, among them, ChBs. Such a chain is depicted in Scheme 1.

Scheme 1. Arrangement of $S(CN)_2$ Molecules in a 1D Infinite Chain with the ChBs Given as Dotted Lines, and Brackets Marking the Repeat Unit

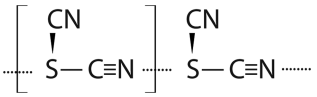

Crystal structures built up from these molecules do exist: there are also experimental reports on $S(CN)_2$[59,60] and $Se(CN)_2$[61−63] (see Figure 1). Both crystal structures were

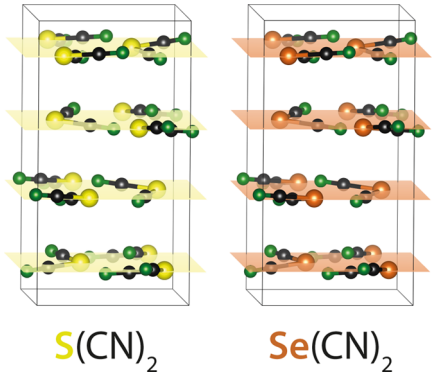

Figure 1. Unit cells of $S(CN)_2$ (left) and $Se(CN)_2$ (right). Structural drawings were created using *VESTA*.[65]

determined in the 1960s; we will revisit both structures here. The main structural motifs of these crystals, however, are not chains but *layers* built up from these chains, as is easily noticeable by looking at the crystal structure. ChBs formed between $S(CN)_2$ and $Se(CN)_2$ molecules have already been computationally investigated by us and others.[22,43,64]

We reoptimized these crystal structures by computation and arrived at the structures analyzed in Table 1. In the case of $S(CN)_2$, the DFT+D lattice parameters are lower than the experimental ones (up to −2%). In the case of $Se(CN)_2$, the DFT-D lattice parameters both underestimate and overestimate the experimental ones (from −2% to +2%). Overall, the bond lengths are both over- and underestimated (up to 4%). To compare the experimental structure with the calculated one, we use the rms of the Cartesian displacement by van de Streek and Neumann (here denoted as "rms*") and, for comparison, the new definition in eq 6 (henceforth, denoted as "rms").[58] As one can see, the experimental structures are in good agreement with the theoretical ones (using van de Streek and Neumann's criterion of rms < 0.25 Å)[58] and vice versa. Moreover, the two definitions do *not* lead to different rms values at this level of accuracy.

Furthermore, we computationally substituted sulfur with oxygen and selenium with tellurium and optimized these hypothetical isotypic structures (see Figure 2). There is a

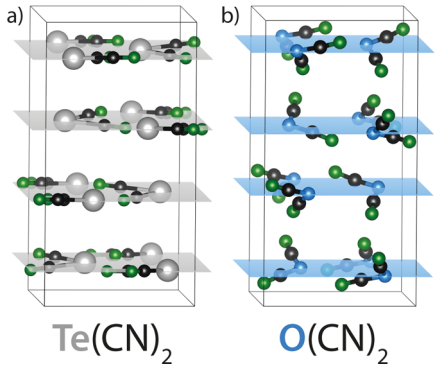

Figure 2. Unit cells of (a) $Te(CN)_2$ and (b) $O(CN)_2$. These hypothetical structures, isotypical to $S(CN)_2$ and $Se(CN)_2$, respectively, are obtained by DFT optimization as described in the text. On the right-hand side, note the significant tilting of the CN units out of the oxygen planes (blue shading).

crystal structure report for $Te(CN)_2$[66] in the literature, but the latter contains solvent molecules and, therefore, has been excluded from the present study. $O(CN)_2$ is, for the time being, a purely hypothetical compound, but we still include it for completeness.

To assess the dynamic stability of these hypothetic structures, we next computed their phonon densities of states (PDOSs), which are given in Figure 3. $Te(CN)_2$ is dynamically stable, whereas the PDOS of $O(CN)_2$ reveals imaginary modes, not unexpected given the nonexistence of the compound thus far. To investigate the PDOSs more precisely, we compare the C−N stretch frequencies to experimental values: The experimental symmetric C−N stretch frequencies[66] in crystalline $Te(CN)_2$ range from 2168 to 2177 cm^{-1}, whereas our computation

Table 1. Comparison of the Experimental Structures of $S(CN)_2$ and $Se(CN)_2$ with the Structurally Optimized Ones

	$S(CN)_2$		$Se(CN)_2$	
	expt[59]	DFT-D	expt[63]	DFT-D
a (Å)	8.56(1)	8.388	8.632(5)	8.449
b (Å)	6.87(1)	6.777	6.847(5)	6.939
c (Å)	12.84(1)	12.679	12.8151(7)	13.100
V (Å)	755.08	720.23	757.41	768.02
d(X−C) (Å)	1.717/1.734	1.695/1.696	1.862/1.870	1.871
d(C−N) (Å)	1.119/1.131	1.169	1.131/1.138	1.168/1.169
d(N···X) (Å)	2.947/2.976	2.841/2.890	2.813/2.835	2.718/2.731
∠C−X−C (deg)	95.76	95.1	91.33	90.13
rms* (Å)	0.04		0.06	
rms (Å)	0.04		0.06	

dx.doi.org/10.1021/ic5023328 | *Inorg. Chem.* 2015, 54, 956−962

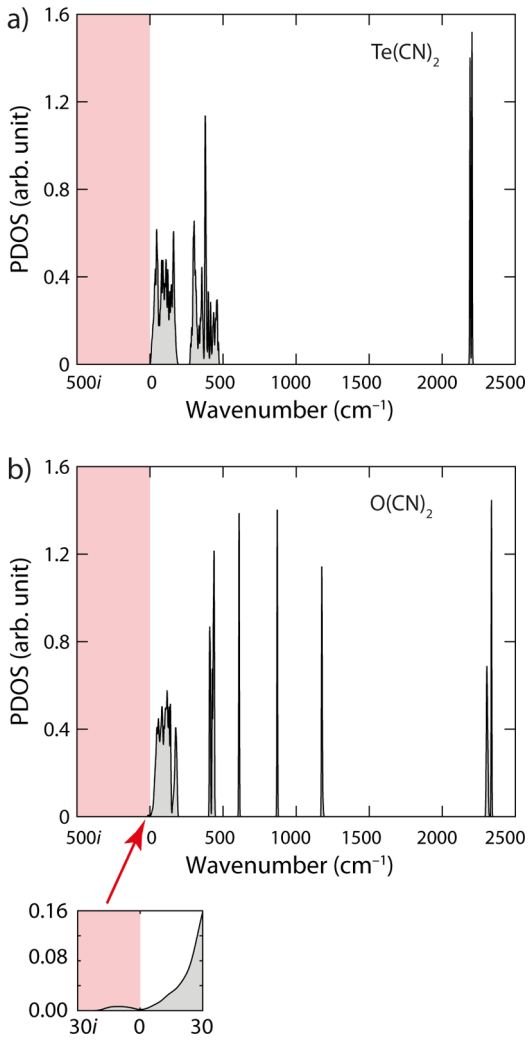

Figure 3. PDOSs of the obtained structures for (a) $Te(CN)_2$ and (b) $O(CN)_2$. The one of $O(CN)_2$ shows a trace of imaginary modes.

reveals frequencies from 2188 to 2206 cm^{-1} for C−N at the Γ point. These values fit well, especially given that the experimental crystal structure and the one used for the computation differ from each other.

A quick look back to Figure 2 reveals that $O(CN)_2$ shows significantly more out-of-plane distortions than the other structures. The CN units are more in the space between the layers than in the other structures. This can be quantified with our above-defined direction-dependent rms of the Cartesian displacement. We calculated the Cartesian displacement vectors and the resulting direction-dependent rms between $X(CN)_2$ (X = O, S, Se, Te) and $Y(CN)_2$ (Y = S, Se, Te), which led to the results given in Table 2. The $S(CN)_2$ and $Se(CN)_2$ structures differ only slightly and thus exhibit the smallest overall rms. In particular, the rms_c value along the *c* axis of the unit cell is diminishingly small. In the case of this orthorhombic crystal structure, the rms_z value is equal to the rms_c value and so on. If one compares $O(CN)_2$ with the other structures, the overall rms value and, most notably, rms_c strongly grows, as one can already guess from the graphic.

To gain better insight into the change *within* the layers compared to that *between* the layers, we further define a rms_{ab} value; that is, we project the rms vector on the *ab* plane, which

Table 2. Direction-Dependent rms of the Cartesian Displacement as Defined in eqs 5, 6, and 8

$X(CN)_2$ compared to $Y(CN)_2$	rms (Å)	rms_a (Å)	rms_b (Å)	rms_c (Å)	rms_{ab} (Å)
X = O, Y = S	0.48	0.19	0.28	0.34	0.34
X = O, Y = Se	0.57	0.19	0.41	0.35	0.45
X = O, Y = Te	0.90	0.29	0.74	0.43	0.79
X = S, Y = Se	0.18	0.07	0.16	0.01	0.17
X = S, Y = Te	0.59	0.22	0.54	0.08	0.59
X = Se, Y = Te	0.43	0.17	0.39	0.08	0.42

is the one containing the molecular layers (shaded in color in Figure 2):

$$rms_{ab} = \sqrt{rms_a^{\,2} + rms_b^{\,2}} \quad (8)$$

All structures differ notably within the *ab* plane, as seen in Table 2, and the change within the *ab* plane (rms_{ab}) is always larger than or similar to the change between the layers (rms_c). This could be a useful tool for analysis of layered structures in future calculations.

Because planes constitute *the* main motif from which the crystal structures are built, we now proceed to isolate dimers, chains, and layers from the crystal; all of this is done in silico and based on fully optimized crystal structures. Then, we compare the interaction energies within these fragments to one another, as depicted in Figure 4.

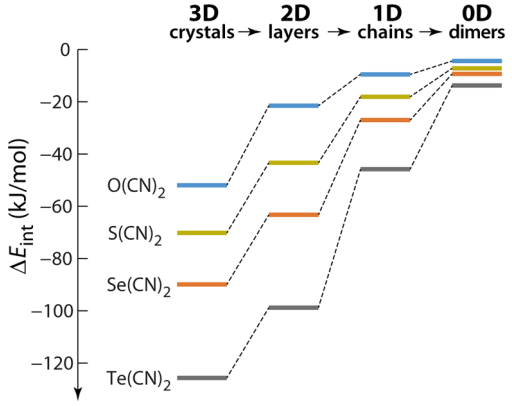

Figure 4. Course of the interaction energies per molecule in the chalcogen cyanide series, following a procedure outlined in ref 45. Gas-phase dimers, chains, layers, and extended crystal structures have been considered.

As expected, the overall interaction energy within the crystal grows from $O(CN)_2$ to $Te(CN)_2$. If one looks more closely, the interaction energy *within* the layers (2D → 0D) grows significantly upon moving from $O(CN)_2$ to $Te(CN)_2$. In the layer, the ChBs are aligned and, therefore, the growth of the interaction energy mainly originates from those. The interaction energy due to layer stacking (3D → 2D) declines from $O(CN)_2$ to $S(CN)_2$, but then it nearly stays constant upon going from $S(CN)_2$ to $Te(CN)_2$. Thus, by contrast, the overall interaction energy growth from $O(CN)_2$ to $Te(CN)_2$ results mostly from the ChBs (i.e., from the 2D → 1D → 0D path). Nonetheless, both the more localized intermolecular interactions *in* the layer, the ChBs, and the less localized interactions *between* the layers play a crucial role for the stability of the crystal. To emphasize this behavior, we plotted the interaction energy within the layer and due to layer stacking

dx.doi.org/10.1021/ic5023328 | Inorg. Chem. 2015, 54, 956−962

separately in Figure 5. The importance of the more localized or the other less localized intermolecular interactions depends on

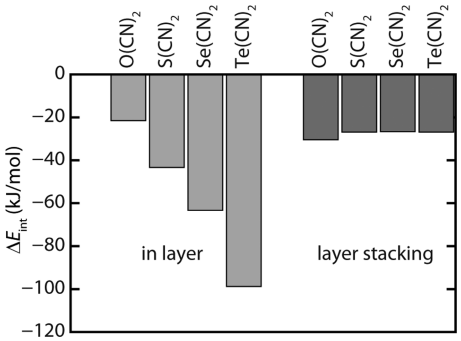

Figure 5. Interaction energies per molecule within the layer and due to layer stacking.

the individual case: The fraction of the in-layer bonding in $O(CN)_2$ is only 41%, whereas it amounts to 79% in $Te(CN)_2$. Overall, this outlines the importance of not only directed intermolecular bonds but also nonlocalized bonding, as already stated by Dunitz and Gavezzotti.[44] We stress that especially $S(CN)_2$ and $Te(CN)_2$ show *very* different contributions in their layered networks (Figure 5), despite the fact that both crystal structures are of very similar appearance (Figures 1 and 2a).

This change in the interaction energy correlates with the structural change identified at the hand of the directionally resolved rms value: The largest change, regarding both energy and structure, occurs within the *ab* plane. The $O(CN)_2$ structure is energetically and structurally most distinct from the others.

Cooperativity in Two Dimensions? Layers as a New Model. The layers have the largest influence on the overall interaction energy in most cases shown, and they are built up from molecules connected by ChBs. Isolated 2D layers, hence, offer themselves as new models to calculate the influence of the ChBs on each other and a possible mutual strengthening, that is, their cooperativity. We have now in silico isolated layers of $O(CN)_2$, $S(CN)_2$, $Se(CN)_2$, and $Te(CN)_2$. Therefore, we cut 2D layers from the crystals of $S(CN)_2$, $Se(CN)_2$, and $Te(CN)_2$ and carefully optimize them in vacuo; doing so constitutes a seamless extension of our previous work,[43] which dealt with the cooperativity in isolated 1D chains. In the case of $O(CN)_2$, we had to computationally substitute the optimized 2D layer of $S(CN)_2$, as before, by replacing sulfur with oxygen. (The layers within the fictional $O(CN)_2$ crystal are structurally too far away from the others so that all optimizations led to a strongly different layer structure in which the $O(CN)_2$ molecules are tilted out of the plane.) To ensure that our layer models represent minima on the potential energy surface, the PDOSs for all four layers were calculated. As was already expected, all layers except $O(CN)_2$ are minima, as identified by the absence of imaginary eigenvalues (exemplarily shown in Figure 6 b). This is in agreement with the behavior for the 3D structures (Figure 3). The most important distances within the layer are presented in Table 3. Not too surprisingly, the X−C distance grows from X = O to X = Te, and the N···X distance falls from X = O to X = Te as the secondary interactions grow stronger. In the case of $Te(CN)_2$, the X−C and N···X distances differ by only 0.54 Å, which nearly questions the definition of the molecular identities.

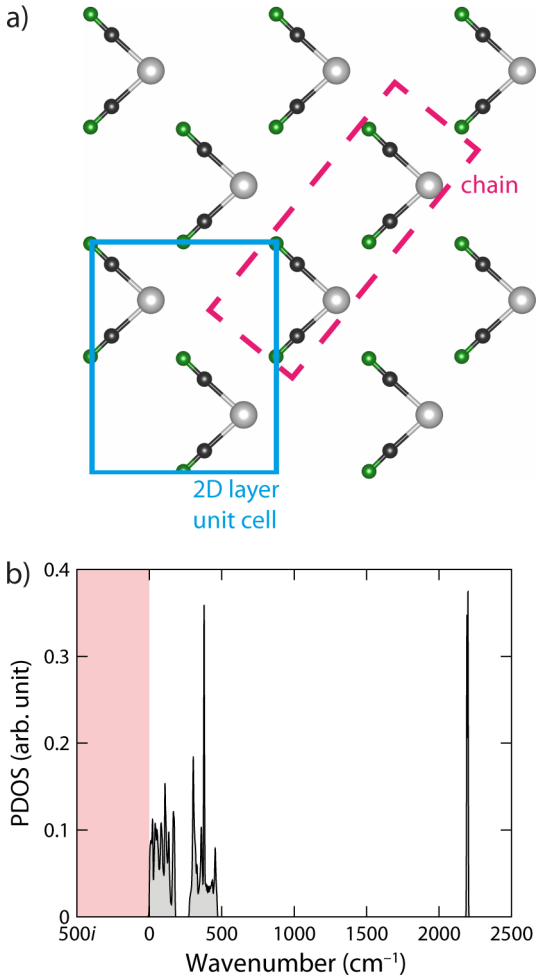

Figure 6. (a) Structurally optimized layer of $Te(CN)_2$ molecules, extending in the paper plane. One chain is also highlighted. (b) Computed PDOSs of the above-shown $Te(CN)_2$ layer. There are no imaginary modes.

Table 3. Interatomic Distances Computed for the Layer Models

	$O(CN)_2$	$S(CN)_2$	$Se(CN)_2$	$Te(CN)_2$
d(X−C) (Å)	1.321	1.701	1.878/1.879	2.111
d(C−N) (Å)	1.166	1.169	1.168	1.169
d(N···X) (Å)	3.07	2.868	2.716/2.717	2.651

Finally, we started with the energetic portioning of the layers. Each molecule within the layer is assumed to have four ChBs to its neighboring molecules. In each chain, one molecule has two ChBs. Interactions with second-nearest neighbors are omitted. Figure 6a sketches the unit cell for the 2D layer (without showing the vacuum region, which would extend perpendicular to the paper plane).

As one can see in Figure 7, the interaction energy per ChB rises from the dimer to the chain to the layer. To be fair, however, there are interactions with the second-nearest neighbors included within the chain and plane so that the overall stabilization energy of one ChB should actually be smaller. To estimate the error introduced by only looking at the nearest-neighbor dimer for comparison, we calculated a chain and a layer of the next-nearest neighbors: In the most extreme case, $Te(CN)_2$, the interaction energy per next-nearest

dx.doi.org/10.1021/ic5023328 | *Inorg. Chem.* 2015, 54, 956−962

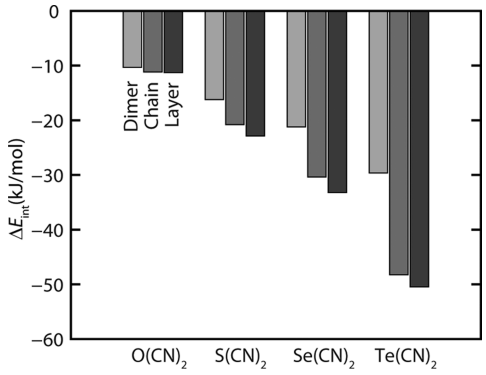

Figure 7. Interaction energies per bond in optimized layers and dimers and chains cut from the layers. Only nearest-neighbor intermolecular interactions are considered; the others are omitted. Note that the interaction energies here are normalized per bond, whereas the interaction energies in the other figures are normalized per molecule.

neighbor in the chain is about 1 kJ/mol (each molecule also has two of such interactions), while in the layer, it is about 6.7 kJ/mol (each molecule also has four of such interactions). If one corrects the interaction energies by this value, there is no rise of the bond-interaction energy from the chain to the plane; instead, one observes a decline of about 2.8 kJ/mol. The chains that constitute the layer are nearly energetically independent: upon formation of 1D chains, the ChBs in these systems are largely cooperative, amplifying each other by up to 62% for $Te(CN)_2$. (Unsurprisingly, the bonds are even more strongly amplified when only the chains are optimized: 90% for $Te(CN)_2$ at the PBE+D2/PAW level of theory.[43]) However, the bonds in the optimized layer are nearly orthogonal during the 1D → 2D step. Energetic orthogonality here means that two intermolecular interactions sharing an acceptor atom do *not* influence each other's interaction energy. This energetic orthogonality was already seen with halogen and hydrogen bonds.[67]

CONCLUSIONS

In this study, we have energetically and geometrically compared layered structures of chalcogen cyanides, as representative model systems for inorganic molecular crystalline networks that are connected by ChBs. We looked at similarities between the orientation of the molecules in the layers via a direction-dependent rms of the Cartesian displacement and, at the same time, at the directionality of the interaction energies via an energetic partition scheme of intermolecular interactions in crystals. Periodic 2D supercells have proven to be suitable ab initio models to study the possible mutual influence of intermolecular interactions in two directions. Applying this model revealed that the chalcogen cyanide layers are built up from chains, which are strongly cooperative within themselves. However, when combined into layers, the ChBs are not further amplified in good approximation (energetic orthogonality). This warrants further research into the assembly of low-dimensional molecular structures and the exploration of their true dimensionality beyond structural arguments alone.

ASSOCIATED CONTENT

Supporting Information

Additional PDOS graphics and optimized structures in the POSCAR format. This material is available free of charge via the Internet at http://pubs.acs.org.

AUTHOR INFORMATION

Corresponding Author

*E-mail: drons@HAL9000.ac.rwth-aachen.de. Fax: +49 (0)241 80-92642. Phone: +49 (0)241 80-93642.

Notes

The authors declare no competing financial interest.

ACKNOWLEDGMENTS

We acknowledge the high-performance computing cluster at the IT Center of RWTH Aachen University for providing large amounts of computing time on the JARA-HPC partition (Project jara0069). J.G. thanks the Fonds der Chemischen Industrie and V.L.D. the Studienstiftung des deutschen Volkes for a scholarship.

DEDICATION

Dedicated to the memory of Prof. John D. Corbett

REFERENCES

(1) Mas-Balleste, R.; Gomez-Navarro, C.; Gomez-Herrero, J.; Zamora, F. *Nanoscale* **2011**, *3*, 20−30.
(2) Novoselov, K. S.; Geim, A. K.; Morozov, S. V.; Jiang, D.; Katsnelson, M. I.; Grigorieva, I. V.; Dubonos, S. V.; Firsov, A. A. *Nature* **2005**, *438*, 197−200.
(3) Zhang, Y.; Tan, Y.-W.; Stormer, H. L.; Kim, P. *Nature* **2005**, *438*, 201−204.
(4) Lalmi, B.; Oughaddou, H.; Enriquez, H.; Kara, A.; Vizzini, S.; Ealet, B.; Aufray, B. *Appl. Phys. Lett.* **2010**, *97*, 223109.
(5) Vogt, P.; De Padova, P.; Quaresima, C.; Avila, J.; Frantzeskakis, E.; Asensio, M. C.; Resta, A.; Ealet, B.; Le Lay, G. *Phys. Rev. Lett.* **2012**, *108*, 155501.
(6) Dávila, M. E.; Xian, L.; Cahangirov, S.; Rubio, A.; Le Lay, G. *New J. Phys.* **2014**, *16*, 095002.
(7) Liu, H.; Neal, A. T.; Zhu, Z.; Luo, Z.; Xu, X.; Tománek, D.; Ye, P. D. *ACS Nano* **2014**, *8*, 4033−4041.
(8) Li, L.; Yu, Y.; Ye, G. J.; Ge, Q.; Ou, X.; Wu, H.; Feng, D.; Chen, X. H.; Zhang, Y. *Nat. Nano* **2014**, *9*, 372−377.
(9) Han, J. H.; Lee, S.; Cheon, J. *Chem. Soc. Rev.* **2013**, *42*, 2581−2591.
(10) Teweldebrhan, D.; Goyal, V.; Balandin, A. A. *Nano Lett.* **2010**, *10*, 1209−1218.
(11) Dickinson, R. G.; Pauling, L. *J. Am. Chem. Soc.* **1923**, *45*, 1466−1471.
(12) Frindt, R. F. *J. Appl. Phys.* **1966**, *37*, 1928−1929.
(13) Ganatra, R.; Zhang, Q. *ACS Nano* **2014**, *8*, 4074−4099.
(14) Feng, J.; Hennig, R. G.; Ashcroft, N. W.; Hoffmann, R. *Nature* **2008**, *451*, 445−448.
(15) Maggard, P. A.; Corbett, J. D. *Inorg. Chem.* **1998**, *37*, 814−820.
(16) Kissel, P.; Murray, D. J.; Wulftange, W. J.; Catalano, V. J.; King, B. T. *Nat. Chem.* **2014**, *6*, 774−778.
(17) Kory, M. J.; Wörle, M.; Weber, T.; Payamyar, P.; van de Poll, S. W.; Dshemuchadse, J.; Trapp, N.; Schlüter, A. D. *Nat. Chem.* **2014**, *6*, 779−784.
(18) Deringer, V. L.; Englert, U.; Dronskowski, R. *Chem. Commun.* **2014**, *50*, 11547−11549.
(19) Steiner, T. *Angew. Chem., Int. Ed.* **2002**, *41*, 48−76.
(20) Metrangolo, P.; Neukirch, H.; Pilati, T.; Resnati, G. *Acc. Chem. Res.* **2005**, *38*, 386−395.
(21) Hassel, O. *Science* **1970**, *170*, 497−502.
(22) Murray, J. S.; Lane, P.; Clark, T.; Politzer, P. *J. Mol. Model.* **2007**, *13*, 1033−1038.
(23) Murray, J. S.; Lane, P.; Politzer, P. *Int. J. Quantum Chem.* **2007**, *107*, 2286−2292.
(24) Murray, J.; Lane, P.; Politzer, P. *J. Mol. Model.* **2009**, *15*, 723−729.

(25) Lommerse, J. P. M.; Stone, A. J.; Taylor, R.; Allen, F. H. *J. Am. Chem. Soc.* **1996**, *118*, 3108−3116.
(26) Riley, K. E.; Hobza, P. *J. Chem. Theory Comput.* **2008**, *4*, 232−242.
(27) Fanfrlík, J.; Přáda, A.; Padělková, Z.; Pecina, A.; Macháček, J.; Lepšík, M.; Holub, J.; Růžička, A.; Hnyk, D.; Hobza, P. *Angew. Chem., Int. Ed.* **2014**, *53*, 10139−10142.
(28) Moilanen, J.; Ganesamoorthy, C.; Balakrishna, M. S.; Tuononen, H. M. *Inorg. Chem.* **2009**, *48*, 6740−6747.
(29) Politzer, P.; Murray, J. S. *ChemPhysChem* **2013**, *14*, 278−294.
(30) Gilli, G.; Gilli, P. *The Nature of the Hydrogen Bond: Outline of a Comprehensive Hydrogen Bond Theory*; Oxford University Press: Oxford, U.K., 2009.
(31) Steiner, T. *Chem. Commun.* **1997**, 727−734.
(32) Grabowski, S. J.; Bilewicz, E. *Chem. Phys. Lett.* **2006**, *427*, 51−55.
(33) Politzer, P.; Murray, J. S.; Concha, M. C. *J. Mol. Model.* **2007**, *13*, 643−650.
(34) Alkorta, I.; Blanco, F.; Elguero, J. *Struct. Chem.* **2009**, *20*, 63−71.
(35) Li, Q.; Ma, S.; Liu, X.; Li, W.; Cheng, J. *J. Chem. Phys.* **2012**, *137*, 084314/1−084314/8.
(36) Esrafili, M. D.; Shahabivand, S. *Struct. Chem.* **2013**, 1−6.
(37) Grabowski, S. *Theor. Chem. Acc.* **2013**, *132*, 1−10.
(38) Solimannejad, M.; Malekani, M.; Alkorta, I. *J. Phys. Chem. A* **2013**, *117*, 5551−5557.
(39) Dominikowska, J.; Palusiak, M. *Chem. Phys. Lett.* **2013**, *583*, 8−13.
(40) Esrafili, M. D.; Vakili, M.; Solimannejad, M. *Chem. Phys. Lett.* **2014**, *609*, 37−41.
(41) Esrafili, M.; Mohammadian-Sabet, F. *Struct. Chem.* **2014**, 1−8.
(42) Alkorta, I.; Blanco, F.; Deyà, P. M.; Elguero, J.; Estarellas, C.; Frontera, A.; Quiñonero, D. *Theor. Chem. Acc.* **2010**, *126*, 1−14.
(43) George, J.; Deringer, V. L.; Dronskowski, R. *J. Phys. Chem. A* **2014**, *118*, 3193−3200.
(44) Dunitz, J. D.; Gavezzotti, A. *Angew. Chem., Int. Ed.* **2005**, *44*, 1766−1787.
(45) Hoepfner, V.; Deringer, V. L.; Dronskowski, R. *J. Phys. Chem. A* **2012**, *116*, 4551−4559.
(46) Deringer, V. L.; Pan, F.; George, J.; Müller, P.; Dronskowski, R.; Englert, U. *CrystEngComm* **2014**, *16*, 135−138.
(47) Kresse, G.; Hafner, J. *Phys. Rev. B* **1993**, *47*, 558−561.
(48) Kresse, G.; Hafner, J. *Phys. Rev. B* **1994**, *49*, 14251−14269.
(49) Kresse, G.; Furthmüller, J. *Phys. Rev. B* **1996**, *54*, 11169−11186.
(50) Kresse, G.; Furthmüller, J. *Comput. Mater. Sci.* **1996**, *6*, 15−50.
(51) Perdew, J. P.; Burke, K.; Ernzerhof, M. *Phys. Rev. Lett.* **1996**, *77*, 3865−3868.
(52) Blöchl, P. E. *Phys. Rev. B* **1994**, *50*, 17953−17979.
(53) Kresse, G.; Joubert, D. *Phys. Rev. B* **1999**, *59*, 1758−1775.
(54) Grimme, S.; Antony, J.; Ehrlich, S.; Krieg, H. *J. Chem. Phys.* **2010**, *132*, 154104.
(55) Moellmann, J.; Grimme, S. *J. Phys. Chem. C* **2014**, *118*, 7615−7621.
(56) Parlinski, K.; Li, Z. Q.; Kawazoe, Y. *Phys. Rev. Lett.* **1997**, *78*, 4063−4066.
(57) Togo, A.; Oba, F.; Tanaka, I. *Phys. Rev. B* **2008**, *78*, 134106/1−134106/9.
(58) van de Streek, J.; Neumann, M. A. *Acta Crystallogr., Sect. B* **2010**, *66*, 544−558.
(59) Emerson, K. *Acta Crystallogr.* **1966**, *21*, 970−974.
(60) Linke, K.-H.; Lemmer, F. *Z. Anorg. Allg. Chem.* **1966**, *345*, 203−210.
(61) Linke, K. H.; Lemmer, F. *Z. Anorg. Allg. Chem.* **1966**, *345*, 211−216.
(62) Fehér, F.; Hirschfeld, D.; Linke, K. H. *Acta Crystallogr.* **1963**, *16*, 154−154.
(63) Klapötke, T. M.; Krumm, B.; Scherr, M. *Inorg. Chem.* **2008**, *47*, 7025−7028.
(64) Alikhani, E.; Fuster, F.; Madebene, B.; Grabowski, S. J. *Phys. Chem. Chem. Phys.* **2014**, *16*, 2430−2442.
(65) Momma, K.; Izumi, F. *J. Appl. Crystallogr.* **2011**, *44*, 1272−1276.
(66) Klapötke, T. M.; Krumm, B.; Gálvez-Ruiz, C. J.; Nöth, H.; Schwab, I. *Eur. J. Inorg. Chem.* **2004**, *2004*, 4764−4769.
(67) Voth, A. R.; Khuu, P.; Oishi, K.; Ho, P. S. *Nat. Chem.* **2009**, *1*, 74−79.